

that using $\gamma=1.7$, the then accepted value, does *not* yield good quantitative agreement with experiment and suggested that better agreement would be obtained with a smaller value of γ . In a further paper¹³ (appar-

¹³ H. Messel, Proc. Phys. Soc. (London) A64, 726 (1951).

ently overlooked by Treiman), Messel presented results adopting "the upper limit $\gamma=1.1$." Instead of the agreement between Messel's theory (with $\gamma=1.7$) and experiment being spurious, the facts are, as stated in the literature, that with $\gamma=1.7$ the theory is not in good quantitative agreement but with $\gamma=1.1$ they are.

The Mechanism of Field Dependent Secondary Emission

HAROLD JACOBS, JOHN FREELY, AND FRANK A. BRAND

Signal Corps Engineering Laboratories, Fort Monmouth, New Jersey

(Received April 3, 1952)

In recent experimental investigations, it was found that secondary emission ratios as high as 10,000 to 1 could be attained utilizing field dependent secondary emission from magnesium oxide. Early tests showed the mechanism causing the high gains to be fundamentally different from the more standard secondary emission phenomenon.

The hypothesis was made that the mechanism of field dependent secondary emission was a process similar to that of the "Townsend avalanche" occurring in gas discharges. As the surface of the dielectric film was bombarded with primary electrons, the high resistivity of the material in combination with the secondary emission current caused the surface to charge to the potential of the collector grid, producing a high field within the dielectric. Electrons released within the material could then gain enough energy to liberate additional electrons, and an avalanche type process resulted.

Experiments were conducted to test this hypothesis and each proved to be consistent with the above theory. The main content

of these experiments can be summarized in the following statements:

(1) The high yields appeared to be independent of the base material. This indicated that the surface or volume effects were most important, implying that a Fowler type field emission from the base metal was not a significant factor.

(2) In studying the secondary current as a function of field, the gas discharge equations were found to be correct. These equations predicted a straight line plot of the $\ln \ln \delta$ vs $1/E$, and in addition, gave a close estimate of the magnitude of the secondary emission ratio.

(3) By means of retarding potential measurements, the energies and mean free paths of the emitted secondary electrons were determined. These data were in good agreement with the results in item (2).

(4) The rise time for surface charging was determined by using square wave variations of bombarding currents, and was found to be consistent with the original hypothesis.

I. INTRODUCTION

IN recent years several workers have reported unusually high secondary emission ratios from thin dielectric films. Their investigations have shown that high dc fields applied across these films cause an enhancement of the secondary emission ratio. In the experiments to be described, high fields were applied across thin films of magnesium oxide while the surface

was being bombarded with primary electrons. The secondary emission ratio was found to increase exponentially with field over a wide range of bombardment energy.¹ By applying a square wave variation of field and observing the rise time of surface charging, it was concluded that the enhanced ratios were the result of a high field created within the magnesium oxide by the charged surface. It was further postulated that secondary electrons, liberated in the material, would be accelerated to such high velocities that an effect similar to the "Townsend avalanche" could occur.

The following discussion is an attempt to explain the mechanism of electron multiplication in the dielectric film.

II. EXPERIMENTAL PROCEDURES

Experimental tubes were constructed as shown in Fig. 1. In this design, C represents an oxide coated cathode to be used as the primary emission source; W indicates the tungsten filaments used for heating the cathode sleeves. G_1 is a negatively biased focusing grid consisting of a disk with a small opening. In some tubes, G_1 was omitted with no noticeable difference.

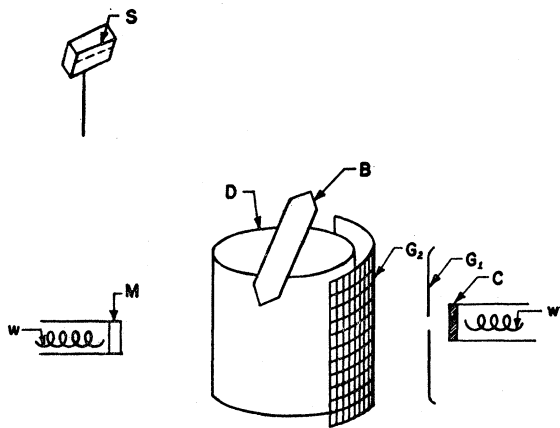


FIG. 1. Experimental tube.

¹ H. Jacobs, Phys. Rev. 84, 877 (1951).

G_2 consists of a wide mesh nickel grid used as both accelerator and collector. The dynode, D, was rotated by an external magnet coupled to shaft B. M represents a high purity magnesium pellet imbedded in a nickel sleeve, and S refers to a shielded barium getter.

The experimental tube was processed in the following manner. At exhaust, the getter, dynode, and grids were degassed and the cathode activated. After admitting oxygen to a pressure of 80μ , magnesium was evaporated onto the dynode. Following this step, the surface was further oxidized by induction heating in approximately 2 mm of oxygen. After the oxygen was removed, the cathode was reactivated, the getter flashed, and the tube sealed and removed from the vacuum system. The magnesium oxide formed on the dynode surface was then rotated in front of the cathode, after which the tube was ready for test. The use of the rotating dynode greatly reduced the possibility of contaminating the secondary emission surface, since during cathode activation the surface was shielded.

It should be emphasized that the magnesium oxide deposit had to be quite porous for best results. Porous layers were obtained by the evaporation of magnesium through this low pressure of oxygen. A smooth deposit resulted when the evaporation was carried out in vacuum, rather than through oxygen. These smooth surfaces were then oxidized by heating the dynode in 2 mm of oxygen. The electrical and mechanical properties of the porous and smooth surfaces were found to be radically different.

When examined microscopically, the surfaces evaporated through oxygen appeared to consist of a uniform distribution of small stalactite structures approximately 6×10^{-4} cm long and 2×10^{-4} cm wide. This surface provided much higher secondary emission ratios and stability. In the case of the deposit carried out in vacuum, the shape of the grains after oxidation was generally more spherical and the size not as uniform. This type of surface did not exhibit field dependent secondary emission, despite all efforts at processing. Both surface types did show a high degree of blue luminescence upon electron bombardment. It was concluded from these experiments that field dependent secondary emission is a structure-sensitive phenomenon, and that the surfaces which showed high ratios were very porous.

The thickness of these deposits was determined to be about 10^{-4} cm by three independent methods, i.e., by microscopic measurement, by means of dielectric breakdown fields, and by decay time observations when the surface was operating as an emitter.

The surfaces were tested using the circuit shown in Fig. 2. The cathode was operated at very low temperatures to prevent barium evaporation,² the bombardment current being of the order of 1 to $10 \mu\text{a}$. With the surface under bombardment, the collector grid was

² H. Jacobs, *J. Appl. Phys.* **17**, 596 (1946); J. B. Johnson, *Phys. Rev.* **73**, 1058 (1948); H. Jacobs, *Phys. Rev.* **85**, 441 (1952).

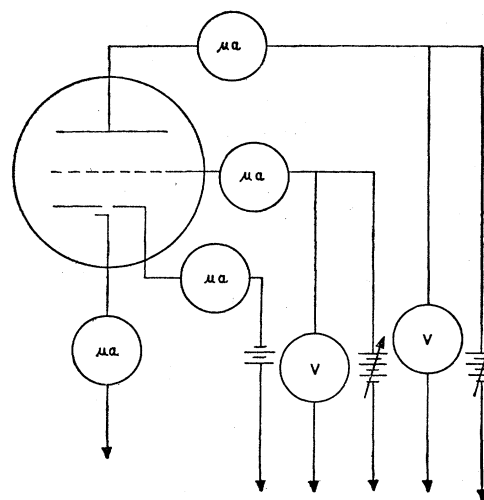


FIG. 2. Static test circuit.

made increasingly positive with respect to the dynode, while measurements were made of the primary and secondary currents. The ratio of secondary to primary current was found to increase nearly exponentially with increasing difference in potential between grid and dynode. Similar results were obtained when the grid potential was kept constant and the dynode voltage lowered, providing the dynode potential was kept over 150 volts. It should be noted that the secondary emission ratios were dependent on the difference in potential between grid and dynode and were independent of bombarding energies above a critical value. This indicates that the high yields were the result of field enhancement.

III. EXPERIMENTAL DATA AND INTERPRETATION

The experiments indicated the following factors to be significant in this investigation:

- (1) The influence of the base material on the magnitude of the secondary current and the durability of the material.
- (2) The dependence of the ratio upon the field within the dielectric film.
- (3) The kinetic energy, internal mean free paths, and collision energies of the emitted electrons.
- (4) The effect of temperature on the ratios.
- (5) The time required for surface charging determined by pulsed bombarding currents.

Since these experimental factors provide the basis for the proposed theory, each item will be discussed in detail.

A. The Role of the Base Material

Tests were conducted with the following dynode base materials: zirconium, tantalum, nickel, barium oxide on nickel, and copper, plated or evaporated on nickel. These experiments showed that variation of the base material had little effect upon the secondary emission properties of the magnesium oxide layers. Figure 3

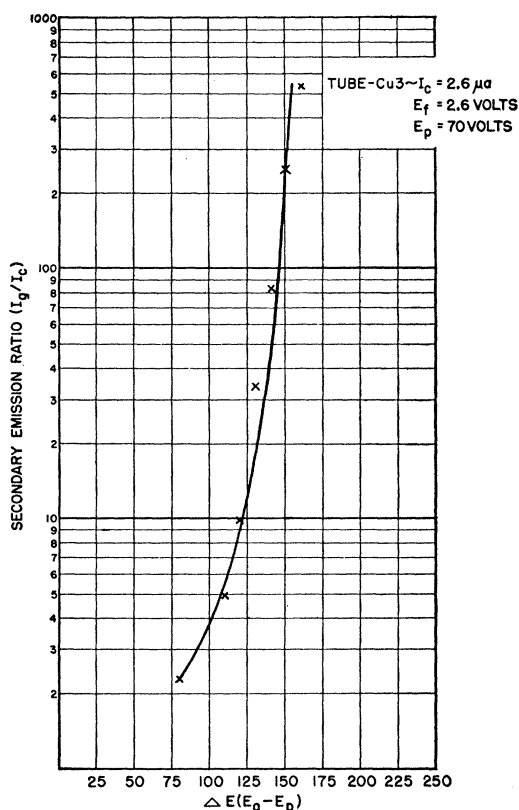


FIG. 3. Secondary emission ratio from magnesium oxide on copper as a function of the potential across the dielectric.

shows the secondary emission characteristics from a dynode which was copper plated and then coated with magnesium oxide. Figures 4, 5, and 6 illustrate similar results from magnesium oxide on pure nickel. Successive tests on the same base material (Fig. 5) showed a greater variation than that from different base materials (Figs. 3 and 4).

The initial secondary emission ratios were evidently independent of base material. However, the power dissipation and lifetime characteristics were found to be quite dependent on the base material. Figure 7 shows the results of a life test using high bombarding currents (1 ma/cm^2). The surfaces with zirconium and barium oxide as base materials would not yield ratios greater than 50 to 1 without arcing. The most durable surfaces were those having nickel as a base material. Life test results with bombarding currents of from 10 to $20 \mu a/cm^2$ are illustrated in Fig. 8.

The fact that the initial secondary emission ratios were independent of the base material indicates that most of the action responsible for the high yields occurs near the surface of the magnesium oxide film since only the material at or near the surface would be chemically similar in all cases. This is a strong indication that field emission from the base material is not a significant factor in the mechanism of field dependent secondary emission.

B. Dependence of Ratio upon Field

In gas discharges there is an effect referred to as the Townsend avalanche.³ When an electron is accelerated through a gas, new electrons are produced according to the relation

$$N = N_0 e^{\alpha x}, \quad (1)$$

where N_0 is the number of initial electrons, x is the distance traveled by the electron from cathode to anode, α is the number of electrons released per centimeter path per electron, and N is the total number of electrons. With field and distance held constant, the ratio N/N_0 will not vary since α is a function of the applied field.

In these experiments the secondary emission ratios were found to be a function of field, and for constant field, the ratios were independent of bombardment current. This led to the hypothesis that the field dependent secondary emission process was similar to the pre-sparking mechanism in a gas discharge. This can be expressed as

$$\delta = i/i_0 = e^{\alpha x}, \quad (2)$$

where i is the secondary current, i_0 is the primary current, δ is the secondary emission ratio, α the number

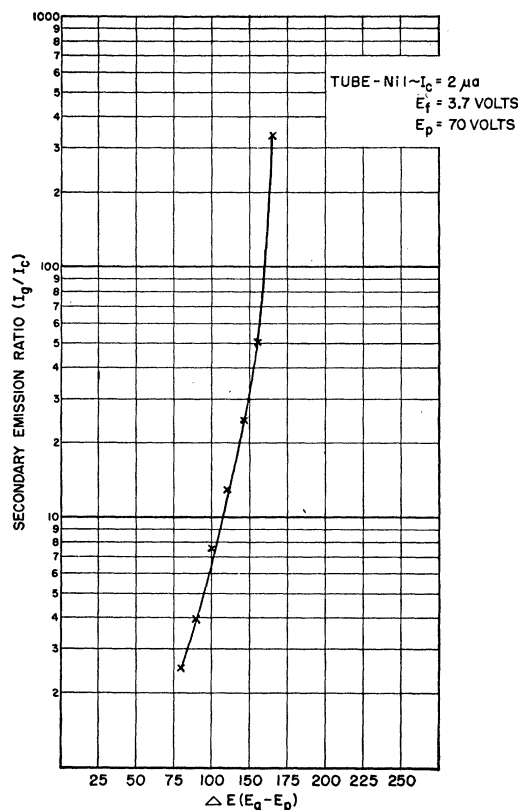


FIG. 4. Secondary emission ratio from magnesium oxide on nickel as a function of potential across the dielectric.

³ L. B. Loeb, *Fundamental Processes of Electrical Discharges in Gases* (John Wiley and Sons, Inc., New York, 1939), pp. 336-370.

of electrons formed per centimeter of path per electron in magnesium oxide, and x is the depth within the material at which the initial secondary electrons are formed.

Physically, one may describe the mechanism of field dependent secondary emission in the following manner. Primary electrons bombard the uncharged magnesium oxide film liberating electrons by ordinary secondary emission with a ratio greater than unity. As a result of its high resistivity, the surface acquires a large positive charge, and a high field is created across the film. Due to the porosity of the film subsequent bombarding electrons will penetrate a fixed distance into the magnesium oxide. Secondary electrons released within the material are now accelerated towards the surface under the influence of the high field. The secondary electrons travel largely through the pores, gaining sufficient energy from the field to create further electrons by impact. Each new secondary electron creates additional electrons by internal ionization, and a Townsend type avalanche results. The limit of gain is finally reached when the surface of the magnesium oxide film approaches the same potential as that of the collector grid. If the surface potential becomes higher than that of the collector grid, the electrons return to the surface, neutralizing some of the positive charges. If the surface falls below the grid potential, the emission of electrons

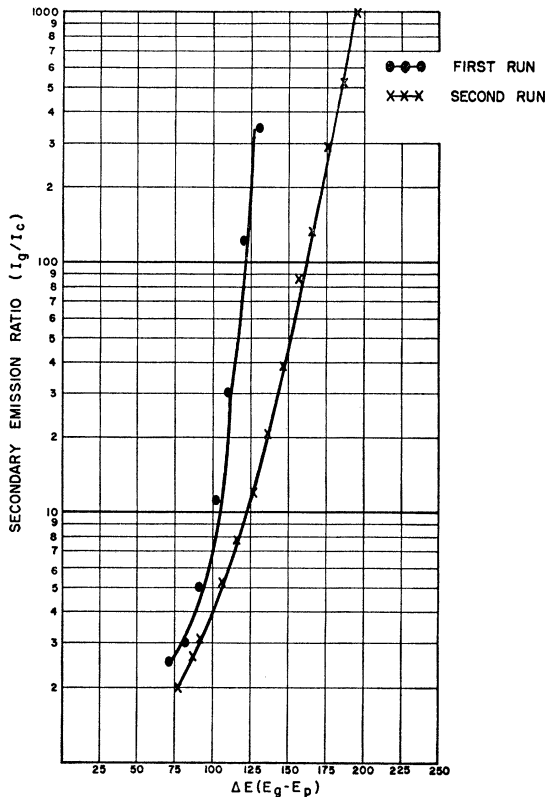


FIG. 5. Secondary emission ratio from magnesium oxide on nickel as a function of potential across the dielectric.

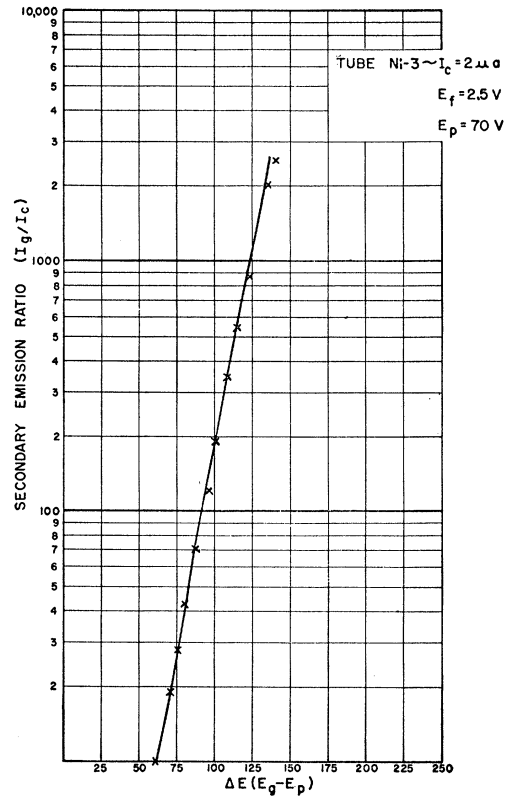


FIG. 6. Secondary emission ratio from magnesium oxide on nickel as a function of potential across the dielectric.

will quickly charge the surface more positively. Therefore an equilibrium potential will be established. The surface of the film thus becomes a unipotential region of positive charges, similar to the condition existing in the cathode glow region of a gaseous glow discharge. This condition implies large mean free paths and mean energies.

An expression for the term α in the factor $e^{\alpha x}$ has been developed by von Engel and Steenbeck⁴ and is given by

$$\alpha = \frac{z}{\bar{v}_e} = \frac{600 p a m}{\bar{v}_e \pi^3 e} C_0^3 e^{-eV_i/kT_e} \left(1 + \frac{eV_i}{2kT_e} \right), \quad (3)$$

where α is the number of electrons produced per cm of path per electron, z is the number of electrons produced per second per electron, p is the pressure, \bar{v}_e is the average electron velocity, e/m is the ratio of charge to mass for electrons, V_i is the ionization potential, T_e is the equivalent electron temperature, k is the Boltzmann constant. C_0 is the most probable velocity, or $2\bar{v}_e/\sqrt{\pi}$, and a is a constant of proportionality. Under conditions of very high fields $eV_i/2kT_e \ll 1$, and Eq. (3) becomes

$$\alpha = A e^{-eV_i/kT_e}, \quad (4)$$

in which A combines the terms preceding the expo-

⁴ See reference 3, p. 368.

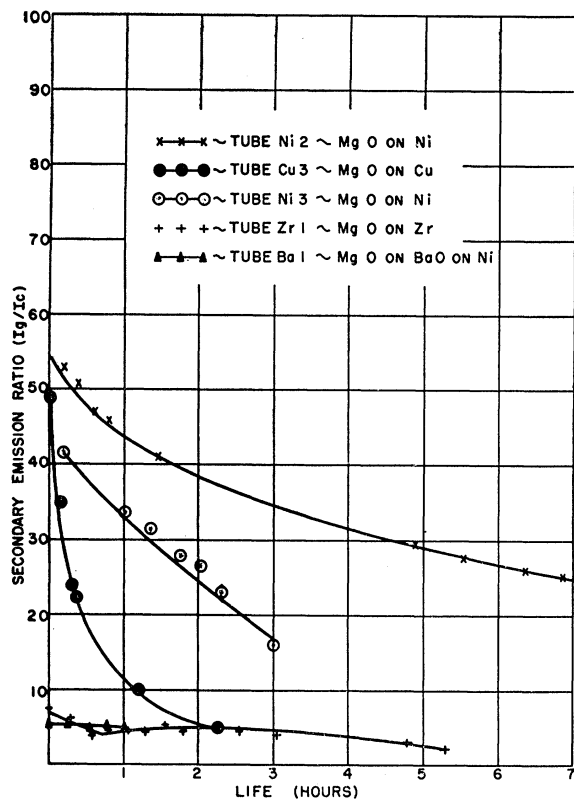


FIG. 7. The decay of the secondary emission ratio as a function of time under conditions of high current density bombardment.

nential and is approximately a constant. If we substitute for kT_e its equivalent in field and mean free path,⁵ it

⁵ The average energy can be expressed by any one of the following equivalent terms:

$$e\bar{E} = \frac{1}{2}m\bar{v}^2 = \frac{1}{2}m[(3/2)v_c^2] = \frac{3}{4}m(\pi/4)\bar{v}_e^2 = \frac{3}{16}\pi m\bar{v}_e^2,$$

where $e\bar{E}$ = average energy, v_c = most probable velocity, \bar{v}_e = average velocity, and \bar{v} = rms velocity. Let us assume that the average velocity can be approximated as

$$\bar{v}_e = (\pi L_e E e / 2m)^{1/2}, \quad (14)$$

where E = field and L_e = mean free path. Using Eq. (14), we find

$$e\bar{E} = (3/2)kT_e = \frac{3}{16}\pi m\bar{v}_e^2, \quad kT_e = \frac{1}{16}\pi^2 L_e E e,$$

or

$$eV_i/kT_e = 1.64V_i/L_e E.$$

Equation (14) is derived under the conditions that the field is strong enough for each collision to be inelastic. That is, the electron starts from rest after each impact, and its terminal velocity is high enough to cause an excited state in the atom with which it collides. For further details, see J. D. Cobine, *Gaseous Conductors* (McGraw-Hill Book Company, Inc., New York, 1941), p. 42.

An alternative derivation of the average velocity, based upon the work of Compton, is described by Loeb (reference 3, p. 368). In this case, the average velocity is determined by

$$\bar{v}_e = (2^{1/2}/\pi^{1/8})[(e/m)EL_e f^{1/2}]^{1/2}, \quad (15)$$

where f = fraction of electron energy lost per collision.

In the limiting case, where $f=1$, all of the electron energy is lost in each collision, and Eq. (15) becomes

$$\bar{v}_e = (2^{1/2}/\pi^{1/8})[(e/m)EL_e]^{1/2}.$$

Numerically then, Eq. (14) and Eq. (15) are in good agreement

follows that

$$eV_i/kT_e = 1.64V_i/L_e E, \quad (5)$$

where L_e is the mean free path and E is the field. Equation (5) then becomes

$$\alpha = A e^{-1.64V_i/L_e E}. \quad (6)$$

Hence, from the Townsend equation, we have

$$\delta = i/i_0 = e^{\alpha x} = \exp(xA e^{-1.64V_i/L_e E}),$$

and

$$\ln \ln \delta = \ln x + \ln A - 1.64(V_i/L_e)(1/E). \quad (7)$$

This equation indicates that if we plot $\ln \ln \delta$ vs $1/E$, the result should be a straight line whose slope is of the same order of magnitude as $-1.64V_i/L_e$. Only the order of magnitude of the slope is predicated since A is only approximately constant.⁶

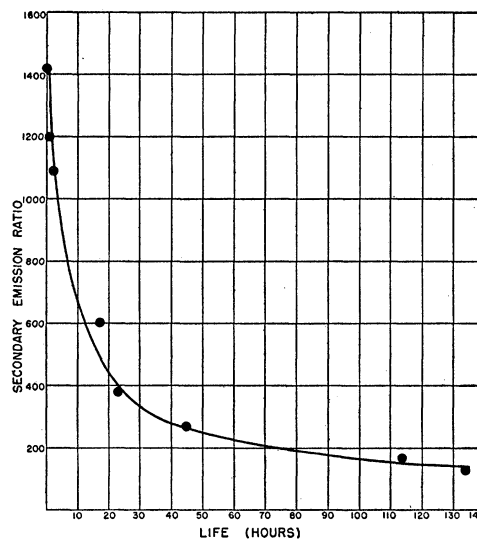


FIG. 8. The secondary emission ratio as a function of time with 10 to 20 microamperes per square centimeter bombarding the surface.

and can be written as follows:

$$\bar{v}_e = 1.25(eL_e E/m)^{1/2} \quad \text{from Eq. (14),}$$

$$\bar{v}_e = 1.03(eL_e E/m)^{1/2} \quad \text{from Eq. (15).}$$

We should prefer to use the derivation and results of Eq. (14), however, since the development is more specific and direct with regard to collisions in the magnesium oxide structure.

We have then made the assumption that the internal energy distribution becomes Maxwellian without a large change in the average velocity (as a result of the density of electrons in the magnesium oxide). This assumption is verified by subsequent experiments.

It might further be added that, using the average velocity of Eq. (14), the equivalent electron temperature can be calculated as,

$$kT_e = 0.610(eL_e E). \quad (16)$$

Using the Compton type equation, the electron temperature becomes

$$kT_e = 0.467(eL_e E), \quad \text{assuming } f=1. \quad (17)$$

The differences in \bar{v}_e and kT_e are not great, and although we have used Eq. (14), either one might have been used to predict the order of magnitude of L_e for Eqs. (6) and (7).

⁶ The error made in assuming that A is a constant amounts to less than 15 percent for gains ranging from 39 to 365; therefore, it is felt that the use of the approximate form does not seriously affect the theoretical development.

TABLE I. Secondary emission and yield.

Field	Secondary emission ratio
4×10^5	2.6
7×10^5	39.0
10×10^5	365.0

In experiments conducted to test this prediction it was found that $\ln \ln \delta$ does vary as $1/E$, as shown in Figs. 9 and 10. To determine E in this case, dielectric breakdown (or arcing) was assumed to start at 10^6 volts/cm. This generally occurred when there was a potential difference of approximately 100 volts across the magnesium oxide. By varying this potential and assuming proportional changes in field, curves were plotted as indicated in Figs. 9 and 10.

Approximate numerical values could be obtained for the ratio V_i/L_e by using the data in Fig. 9 and rewriting Eq. (7) as

$$\frac{\ln \ln \delta - \ln \ln \delta'}{1/E - 1/E'} = 1.64 \frac{V_i}{L_e} \quad (8)$$

Substituting experimental values, we find that

$$L_e = 0.205 V_i \times 10^{-5} \quad (9)$$

If we assume $V_i \cong 10$ ev, then $L_e \cong 2 \times 10^{-5}$ cm. For the

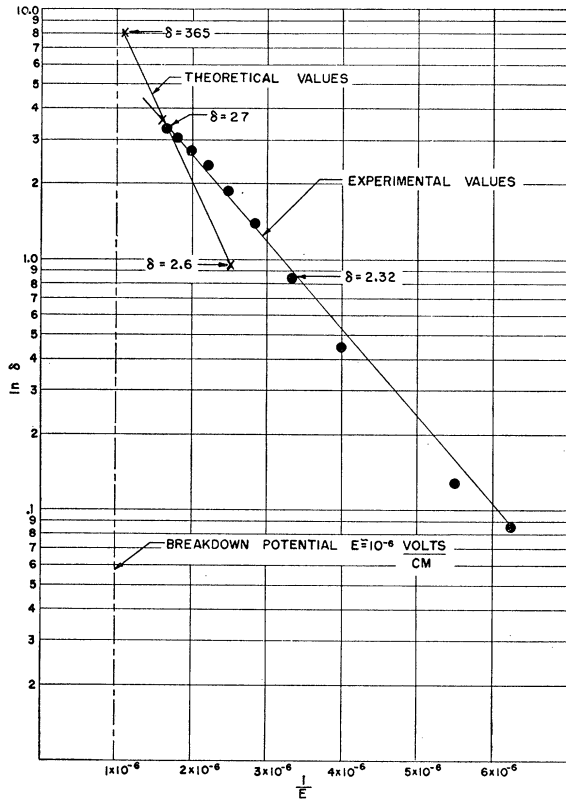


FIG. 9. The $\ln \ln$ of the secondary emission ratio as a function of the reciprocal of the field.

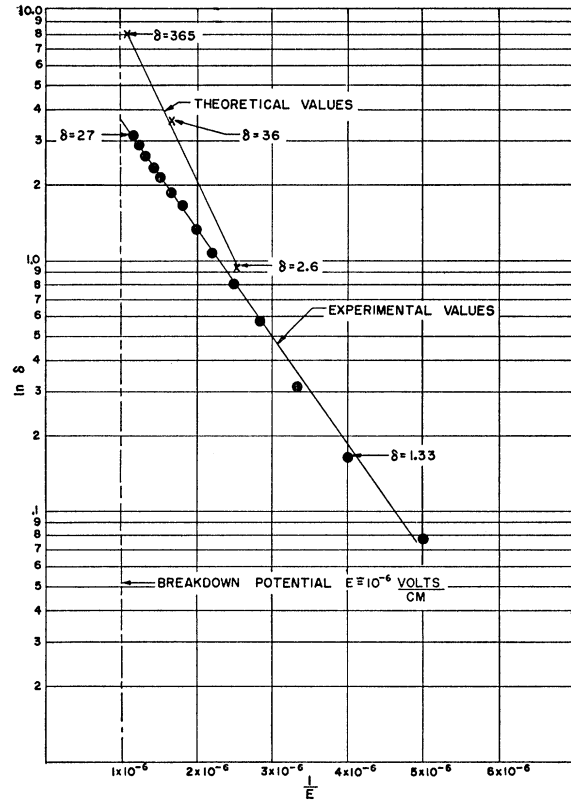


FIG. 10. The $\ln \ln$ of the secondary emission ratio as a function of the reciprocal of the field.

case of Fig. 10, $L_e \cong 1.6 \times 10^{-5}$ cm. These values are in good agreement with those obtained independently by retarding potential measurements, where $L_e \cong 1.1 \times 10^{-5}$ cm.

In addition to predicting a slope, the actual value of the secondary yields can be estimated and shown to be close to the experimental values by referring back to the von Engel and Steenbeck equation,

$$\alpha = \frac{z}{\bar{v}_e} = \frac{600 p a m}{\bar{v}_e \pi^3 e} C_0^3 e^{-eV_i/kT_e} \left(1 + \frac{eV_i}{2kT_e} \right) \quad (3)$$

Assume $E \cong 10^6$ volts/cm, $L_e \cong 10^{-5}$ cm, $a \cong 1$, $p = 4 \times 10^5$ mm (the pressure corresponding to a mean free path of 10^{-5} cm in nitrogen), $eV_i = 5$ ev, $kT_e = \frac{1}{16} \pi^2 L_e E$, and $\bar{v}_e = (\pi L_e E e / 2m)^{1/2} \cong 1.6 \times 10^8$ cm/sec. If we now substitute the above factors in Eq. (3), we find that $\alpha = 5.9 \times 10^4$. Since breakdown occurs with approximately 100 volts applied across the film, and assuming $E = 10^6$ volts/cm for dielectric breakdown, we find that the film thickness, x , is 10^{-4} cm and

$$\delta = e^{\alpha x} = 365 \text{ gain.} \quad (10)$$

Values of δ calculated at this and other fields are shown in Table I. These calculated values are indicated on Figs. 9 and 10 and are in fairly good agreement, with the experimental data, if we consider that V_i and

L_e were only approximated. By changing these values slightly, the slope could readily be adjusted to fit the observed values.

C. The Energy of Emitted Electrons and Retarding Potential Measurements

A tube employing retarding potential principles was designed to analyze the energy spectrum of the emitted electrons (Fig. 11). The grid consisted of a solid sheet with two openings; one allowing the primary beam to enter, and the other permitting a portion of the emitted secondaries to pass through to the collector. Secondary emission from the collector was prevented by coating its inner surface with carbon black. Electron trajectories were determined by dusting the tube parts with willemite. Although it appeared that the primaries struck the magnesium oxide surface in a finely defined spot (about 0.01 cm²), the secondaries were emitted from a much larger area of the film (0.3–0.5 cm², depending on the field).

Some of the electrons leaving the magnesium oxide surface passed through the second opening and were recorded at the collector as various retarding potentials were applied.

A distribution of electron energies was determined by plotting the number of electrons per unit energy range as a function of energy, and from this data, an estimate of the average energy could be made. This average energy \bar{E} of the emitted electrons was found to range between 10 and 20 ev.

A knowledge of the average electron energy allows an estimate to be made of the mean free path, which can then be checked with the values predicted in part B. Assuming that the energy distribution of the electrons on leaving the surface is the same as within the material, it follows that

$$e\bar{E} = (3/2)kT_e = \frac{3}{16}\pi m\bar{v}_e^2, \quad (11)$$

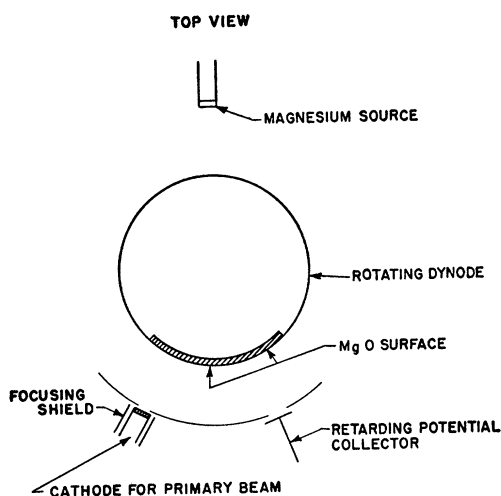


Fig. 11. Experimental tube structure for studying the energy of emitted electrons utilizing retarding potentials.

and

$$\bar{v}_e = (\pi L_e E e / 2m)^{1/2} \text{ esu,}$$

or

$$e\bar{E} = \frac{3}{16}\pi^2 L_e E e. \quad (12)$$

Let $e\bar{E} = 10$ ev, the average energy of the electron, and $E = 10^6$ volts/cm, the field across the dielectric. By substituting these values into Eq. (12), we obtain $EL_e \cong 11$ ev, or $L_e \cong 1.1 \times 10^{-6}$ cm.

The estimates of the mean free paths given by the retarding potential method are in good agreement with the values estimated by the method described in part B, where the ratios were determined as a function of electric field.

As a refinement of the retarding potential measurements, the natural logarithm of the collector current was plotted *versus* the retarding potential in a procedure similar to that used for probe studies in a plasma.⁷ From these plots one observes a linear dependence on energy (indicating a Maxwellian energy distribution), and from the slope a value for the average energy may be determined. The true surface potential is also indicated by methods similar to those measuring contact potentials, making possible a more quantitative determination of the field across the film. The average energy, determined from such plots was found to be approximately 11.1 ev, and the mean free path approximately 1.1×10^{-5} cm. Therefore, the values obtained for the mean free path and average energy, by three independent methods, are found to be in good agreement.

D. The Variation of Ratio with Temperature

The secondary emission ratio was found to be relatively unaffected by variations in temperature. The experiment was performed by placing the entire tube in an oven and observing the primary and secondary currents while slowly raising and lowering the temperature. (The rate of change was approximately 50°C per hour.) It was found that, in general, the ratio decreased somewhat with rising temperature and increased with falling temperature returning to approximately its initial value, as shown in Fig. 12.

E. Rise Time Effects

If our picture of the mechanism of field dependent secondary emission is correct, the yield should show a finite rise time. This time lag results from the fact that with a sudden increase in field, or current, the surface must charge to a new equilibrium. According to McKay,⁸ the rate of charging of an insulator can be calculated as follows:

$$E = [(\delta - 1)/K] j_p t \times 1.13 \times 10^{13} \text{ volts/cm,} \quad (13)$$

where t = time; j_p = bombardment current, amp/cm²;

⁷ See reference 3, p. 240.

⁸ K. G. McKay, *Advances in Electronics* (Academic Press, Inc., New York, 1948), Vol. 1, p. 109.

and K =dielectric constant. For relatively low ratios, i.e., $\delta=4.5$, $j_p=10^{-5}$ amp/cm², where $K=3.5$ and $E\cong 10^6$ volts/cm, we find that $t=10^{-2}$ second. Similarly, for $\delta=3500$, $t=10^{-5}$ second before equilibrium is established.

If we apply this concept to the magnesium oxide surfaces, bombarded with a square wave pulse of primary current, we should expect the following results. If there were no previous charge on the surface (as exists, for instance with no dc bombardment current) the initial secondary emission ratio would be low, and the charging of the surface to equilibrium might require a relatively long time, 10^{-2} to 10^{-3} second. However, if a dc bombardment has been present prior to an increase in bombardment current, the field across the dielectric would already be present and the initial ratios would be higher, i.e., 3500 to 1 rather than 4.5 to 1. This higher ratio would then decrease the time lag by a factor of 10^3 , for the new equilibrium to be reached.

Rise time experiments were performed to investigate the conditions mentioned above, and the values predicted by Eq. (13) were found to be quite close to the experimental results.

With a steady state gain of about 130 to 1, $j_p=12 \times 10^{-5}$ amp/cm², and $E\cong 10^6$ volts/cm², the calculated rise time was 1.7×10^{-5} second. The observed rise time under these conditions was approximately 2.0×10^{-5} second. It was further noted that the rate of rise increased both with field and bombardment current.

Square wave variations of primary current were also made with no initial dc bombardment, and the time lags were found to be greater. For a value of $\delta=70$ after equilibrium, $E\cong 10^6$ volts/cm, and with $j_p=4.4 \times 10^{-6}$ amp/cm², the rise time was calculated to be 2.0×10^{-3} second. Experimentally, the time for equilibrium to be reached was found to be 1.6×10^{-3} second under these conditions. Experiments of this type indicate that the rise time of surface charging can be decreased by increasing the bombardment current, or by maintaining a high field across the surface so that δ is kept high.

IV. CONCLUSIONS

The mechanism of field dependent secondary emission can be described as follows. As a result of conventional secondary emission, the bombarding electrons tend to charge the surface of the dielectric positively creating a high field across the film. Due to porosity (an essential factor in obtaining these high yields), most of the

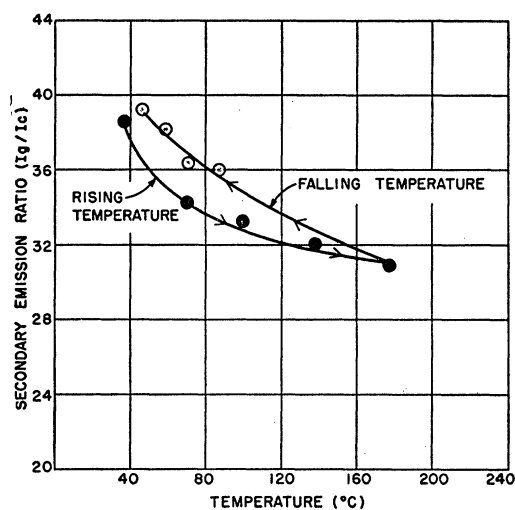


FIG. 12. The secondary emission ratio of magnesium oxide as a function of temperature.

primary electrons can penetrate some distance into the volume of the dielectric releasing secondary electrons. The secondaries, in turn, are accelerated toward the surface of the film, and at sufficiently high fields an electron avalanche will occur.⁹

The mean energy of the emitted electrons is roughly 10 to 20 ev and the mean free paths of the secondaries within the dielectric are approximately 10^{-5} cm. Several independent experiments were found to lead to the same conclusions. These include the variation of secondary emission with field, the use of retarding potential measurements, and the measurement of rise times with varying bombarding currents.

Acknowledgment should be made to Dr. J. E. Gorham and Dr. D. Dobischek of the Signal Corps Engineering Laboratories, to Professor A. Van der Ziel of the University of Minnesota and to Dr. E. M. Baroody of Battelle Memorial Institute for their advice during the course of this work.

⁹ Considerable theoretical work has been done recently on the mechanism of dielectric breakdown and electron multiplication in solids. [See F. Seitz, Phys. Rev. **76**, 1376 (1949); H. B. Callen, Phys. Rev. **76**, 1394 (1949); H. Frohlich, Phys. Rev. **61**, 200 (1942).] Unfortunately, the emphasis in these works has been on single crystal effects only, and little mention has been made regarding such effects in polycrystalline, nonhomogeneous media. Hence, the concepts and equations developed in these theories do not have a suitable application in the present discussion, where, it is felt, the prime factor is film porosity and not a crystalline breakdown.